Short Circuit and Induced Voltage Transient Study on a Planned 1000 MW HVDC-VSC Cable Link

L.Colla, S. Lauria, F.Palone

***Abstract* – TERNA, the Italian TSO, is planning new HVDC interconnections with neighboring countries including underground links based on VSC technology; short circuit transient studies of such links require accurate cable line modeling in a frequency range from dc to 10 kHz at least. The finite section approach was used to this purpose. Short-circuit transient simulation results evidenced significant temporary overvoltages following a single pole-to-earth cable fault, due to unfaulted cable charging by free-wheeling diodes has been evidenced in the study. Results are in good agreement with theory and proved to be also useful for evaluating the induced voltage on nearby communication cables and to evaluate the possible application of surge arresters.**

***Keywords*: HVDC, short-circuit, transient studies, current distribution, induced voltage, cable model, finite sections, ATP-EMTP.**

I. Introduction

TERNA is currently planning a new 200 km long HVDC international interconnector [1], entirely made of underground cables. In the course of the feasibility study, TERNA examined one Voltage Source Converter (VSC) option without dc side capacitors or smoothing reactors, and with ac neutral not effectively grounded on the converter side of interface transformers. Normal operation of VSC converters involves several valve commutations for cycle of network frequency, following a given voltage/current control pattern; during short-circuits, however, valves are blocked and current only flows through free-wheeling diodes until ac circuit breakers trip on both sides of the link.

A study of the short circuit transient was needed, in order to evaluate the magnitude of fault currents and their effect on the nearby communication/safety circuits. An EMTP model of the dc link [2] under faulted condition was developed to this purpose, using ATPDraw [3]. Finite Sections (FS) technique [4] was used since a wide-band cable model was required in a study involving frequencies ranging from dc to rectifier characteristic harmonics, plus the impulsive cable discharge. The model consists of cascaded multi-conductor "enhanced pi" cells where constant parameters, lumped R-L ladder networks reproduce current distribution within each conductor and in the ground.

S. Lauria is with the Dept. of Astronautics, Electrical and Energetics Engineering, University of Rome "Sapienza", via Eudossiana 18, 00184 Rome, Italy (stefano.lauria@uniroma1.it).

L. Colla and F. Palone are with TERNA S.p.A., Grid Development and Engineering, via Galbani 70, 00156 Rome, Italy (e-mail luigi.colla@terna.it, e-mail of corresponding author: francesco.palone@terna.it).

Paper submitted to the International Conference on Power Systems Transients (IPST2011) in Delft, the Netherlands June 14-17, 2011

Longitudinal coupling by lossless inductive arrays and appropriate R-C shunt networks complete an individual cell assembly, accounting also for dielectric losses and semi-conductive layers. Pipe/tunnel installation and earth stratification can also be included. A comprehensive description of the FS technique is given in [4] and in the companion paper [5]. Given their very low probability of occurrence, faults affecting both poles were not considered: simulations were focused on single core-to-sheath faults, investigating the short circuit current magnitude, duration and its distribution between cable sheaths and ground. Induced voltages on nearby auxiliary and safety LV circuits were also computed.

II. System Description and Modeling

The considered 200 km long HVDC link will actually consist of two independent ±320 kV multilevel VSC systems, each rated 500 MW, as shown in the single-line diagram of Fig. 1. The short circuit study was carried out for one link, as the installation of the second is foreseen at a later time.

The 320kV HVDC lines are entirely underground with one 2500 mm^2 Al XLPE-insulated cable per pole; the four cables run together for the whole length of the link, which includes 13 km of tunnel installation.

The preliminary project does not have smoothing reactors or dc side capacitors external to the converters, and there is no intentional dc grounding in the converter stations. On the ac network side the neutral of wye-delta converter transformers is solidly grounded; on the converter (delta winding) side of the transformers, neutral is high impedance grounded (at one terminal station of the HVDC link only) via a star point reactor. The interconnected 400kV 50 Hz networks have been conservatively simulated by 63 kA fault (Thévenin) equivalents, with a X/R ratio of 15. Converter transformers, 400 kV/440 kV, rated 500 MVA, with 16% short circuit impedance, have been represented by the ATP-EMTP SATTRAFO model [3][6].

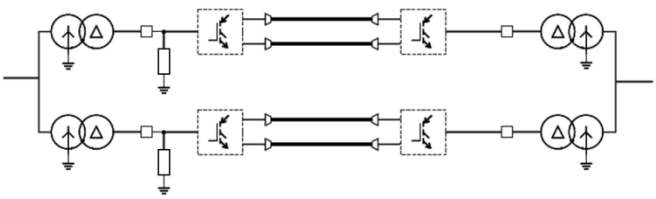

Fig. 1. HVDC system representation at final installation stage

For dc short-circuit simulation purposes each multi-level converter is represented only by its free-wheeling diodes,

avoiding detailed valve simulation (actual VSC protective arrangement, based on "crowbar" thyristors should not change this behaviour). An ATPDraw schematic of the studied system is represented in Fig. 2. The cables are 2500 mm^2 Al with aluminum sheaths and XLPE insulation. Electrical and geometrical data are reported in Fig. 3, which also shows laying arrangement for direct buried portion of one link, i.e. at 1.2 m depth in a 500 Ωm ground. Cable sheaths are earthed at both terminals and every 5 km on independent ground rods. All ground connections have been explicitly represented, along the FS cable model; the 13 km long tunnel installation has been straightforwardly simulated within the FS model itself [2].

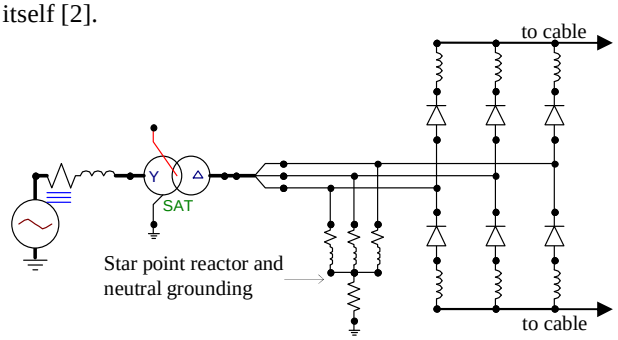

Fig. 2. ATPDraw sketch of the simulated converter station.

III. DC SHORT-CIRCUIT CURRENT CALCULATION

Single pole-to-sheath faults were considered to occur either at the middle (case A) or at the end of the dc cable (case B). The steady state fault current is kept at very small values by the absence of dc grounding and the high impedance ac neutral grounding on the converter side of transformers. The peak value of transient short circuit current due to cable discharge, however, does not depend on ground path impedance but only on cable electrical characteristics and as such can attain much higher values.

To a first approximation, initial cable discharge current I_i is given by

$$I_i = \frac{E}{Z_c} \qquad (1)$$

being E the pre-fault pole voltage to ground and Z_c the coaxial wave impedance of the cable:

$$Z_c \cong \sqrt{\frac{L'}{C'}} \qquad (2)$$

Where L' and C' are the core-to-sheath inductance and capacitance, i.e. the relevant parameters of the coaxial propagation mode. Wave impedance actually depends on frequency, being both longitudinal impedance and admittance complex functions of the frequency; in addition, as the coaxial propagation mode is not the only one involved in the discharge phenomenon, the actual discharge current is a sum of modal components. However, due to its high frequency content, most of the discharge current recloses in the faulted cable sheath so that (1) gives an acceptable approximation. With a pre-fault voltage E = 320 kV between conductor and cable sheath, considering Z_c =19.1Ω for the cable in question, the peak discharge current I_i according to (1) is 16.8 kA. If the fault occurs in an intermediate section of the cable, the peak value of the fault current is $2I_i$ due to contribution of two discharging currents waves from both sides.

ATP-EMTP simulation results are well matched with these preliminary calculations as can be seen in Fig. 4 where simulated fault currents are reported. Short circuit current peak value is 35 kA if the fault occurs in the middle of the line and 17 kA if the fault occurs at the end of the line, fully in agreement with (1). The difference (<5%) can be ascribed to the approximation in calculating Z_c and to the lumped nature of the Finite Sections equivalent circuit. In both cases steady-state short circuit current does not exceed 150 A rms.

The simulation does not take into account converter control, whose behavior modifies significantly the steady-state current, but should not affect peak current value.

320kV dc, 2500 mm^2 Al, XLPE insulated cable

Geometric data	
Conductor radius	31 mm
Inner semicon thickness	2 mm
Insulation thickness	18 mm
Outer semicon thickness	3.2 mm
Metallic sheath width	1.2 mm
Total diameter	111.6 mm
Typical laying data	
Laying distance (D)	200 mm
Laying depth (h)	1200 mm
Electric data	
DC resistance at 20°C	12 mΩ/km
Capacitance	309 nF/km

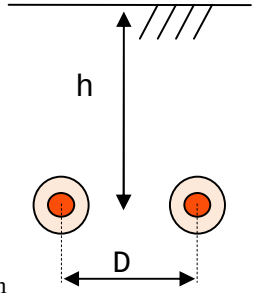

Fig. 3. Cable system description, for one of the HVDC links in Fig. 1.

The mean value (i.e. dc component) of short-circuit permanent current is 33 A for both cases (mid-line and line-end fault). Ac components, which circulate also through cable capacitance, depend on fault location as can be seen in Fig. 5. The ac component of permanent short circuit current (mainly 6th harmonic current, as shown in Fig. 6 and Fig. 7) is considerably larger than dc for both studied fault location. Cable terminal currents (at the station with the star point reactor), shown in Fig. 8 for a mid-line fault occurring at t = 0.2 s, are similar for both the studied cases.

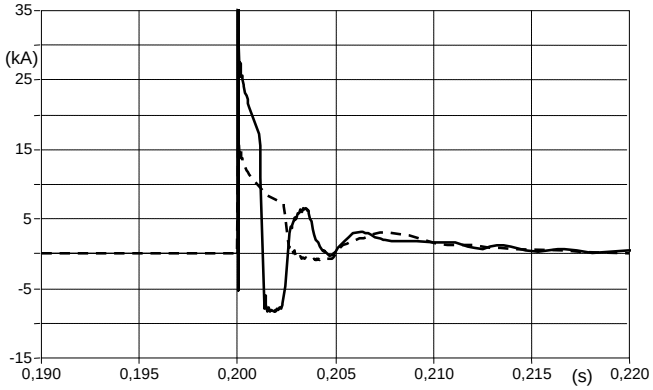

Fig. 4. Simulated core-to-sheath short-circuit current, vs time: initial transient of mid-line fault (solid line), and line-end fault (dotted line). ±320 kV pre-fault dc line voltage; fault inception at t=0,2 s.

As the HVDC control system has not been taken into account, the simulated fault current waveform does not

practically change, once the initial discharge is over; in actual operation, fault clearing by ac circuit breaker opening should normally occur within 100 ms.

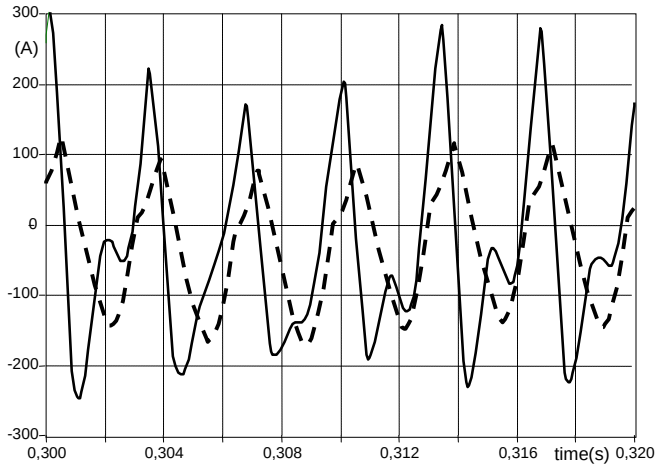

Fig. 5. Simulated core-to-sheath short circuit current vs. time: steady-state current for mid-line fault (solid line), and line-end fault (dashed line). Initial condition as in Fig. 4

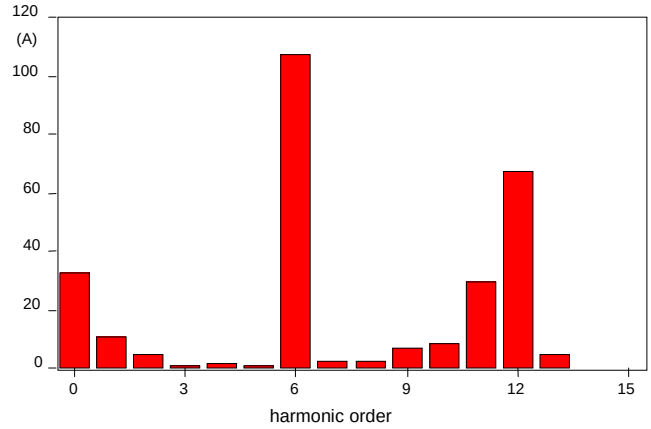

Fig. 6. Harmonic analysis of steady-state, mid-line fault current (solid line in Fig. 5), RMS values.

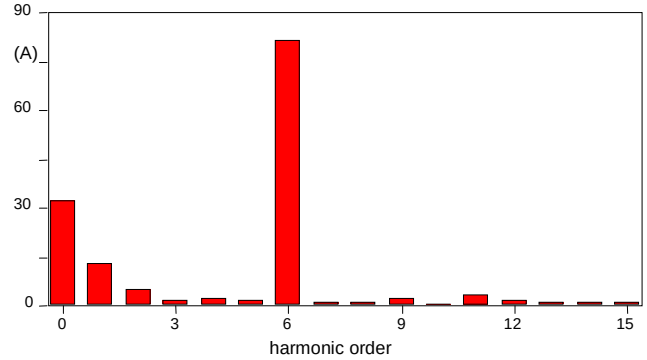

Fig. 7. Harmonic analysis of steady-state, line-end fault current (dotted line in Fig.5), RMS values.

IV. Fault Current Distribution Between Cable Sheaths and Ground

The determination of the actual fault current distribution between the metallic sheath of the faulted cable and ground is of paramount importance for the calculation of induced voltage on nearby circuits, according to present standard procedures [7].

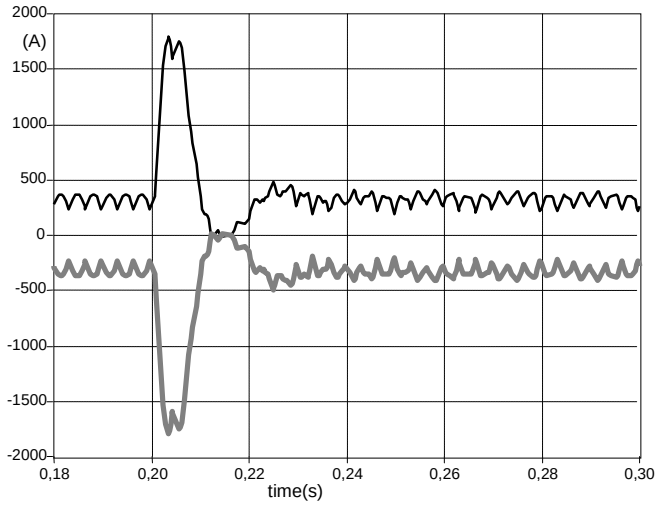

Fig. 8. Current at the dc busbars for a mid-line fault; positive pole (black) and negative pole (thick grey line).

This is immediate when using the FS model, which explicitly represents all cable system conductors including the ground return path. Fig. 9 shows the current distribution at fault point, for a mid-line fault: at the beginning of cable discharge most of the current interests only the faulted cable sheath, whereas during the following oscillations the current distributes more evenly between the two cables' sheaths. It is noticeable that almost only dc current flows in the ground rod.

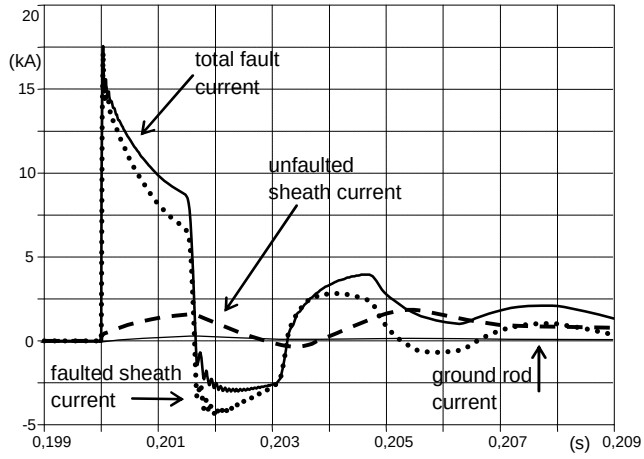

Fig. 9. Sharing of line-end fault current (see Fig. 4, solid line), among different return paths, vs time: total current: thick solid line, faulted cable sheath current: dotted line, unfaulted cable sheath current: dashed line, ground rod current: thin solid line.

V. AC Side Currents

The simulated multilevel VSC scheme is not provided with ac harmonic filters: as a consequence operation with blocked valves (i.e. as an uncontrolled six-pulse Graetz bridge) is associated to heavily distorted ac side current waveforms, as shown in Fig. 10. Characteristics ac harmonics of the 6-pulse converter, i.e. current harmonics of order 6n±1, mostly 5th and

7th, are clearly recognizable in the reported waveforms. This is confirmed by Fourier analysis of the steady-state portion of Fig. 10, shown in Fig. 11; large 5th and 7th harmonic distortion is clearly visible, with smaller but significant 10th, 11th and 13th harmonics as well.

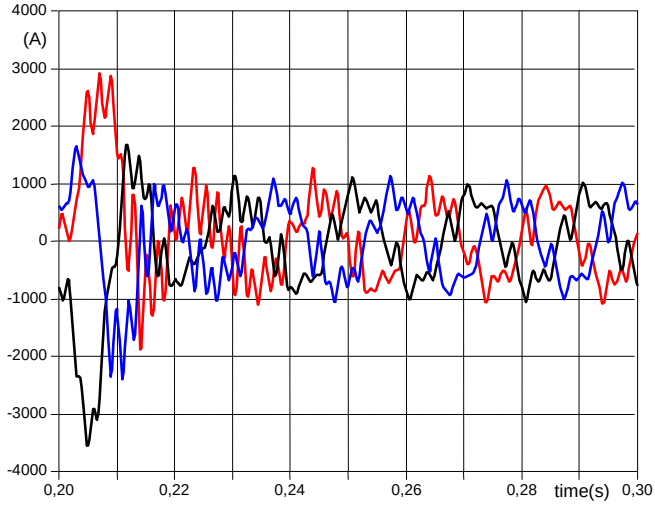

Fig. 10. AC line currents on the primary (network) side of converter transformer, vs time, for a near line-end fault occurring at t=0.2.

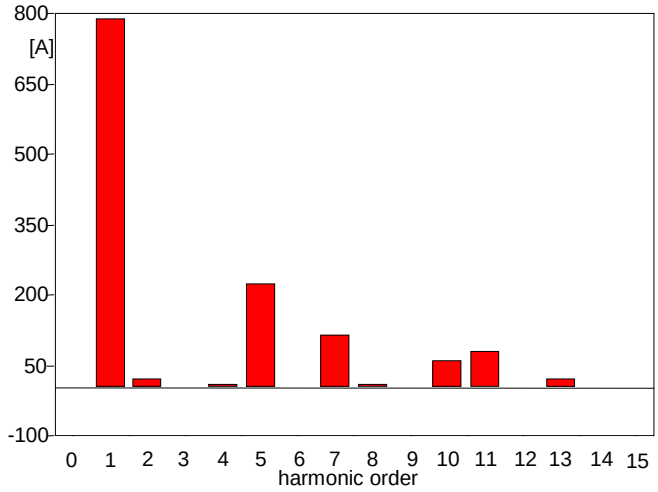

Fig. 11. Harmonic analysis of the R phase ac line current in Fig. 10.

VI. Converter Station Voltage

Since neither converter controls nor protective devices and manoeuvres are simulated, the faulted pole voltage quickly drops to zero; on the other hand the absence of intentional grounding on the dc side of the converter causes an increase of the healthy pole voltage to ground, up to the whole rated pole-to-pole voltage (i.e. 2×320 kV), as shown in Fig. 12. This can be regarded as a temporary overvoltage since it lasts until the fault current is interrupted by circuit breakers opening at both terminal stations (after 100 ms at least), and must be taken into account for the insulation coordination of cables and converters. The severe healthy pole overvoltage could be mitigated by Metal Oxide Surge Arresters (MOSAs) connected between each pole and ground. ATP-EMTP fault simulations were thus repeated with the addition of MOSAs, represented by Type 99 non-linear resistors, adopting the V-I characteristic of commercially available station-class arresters.

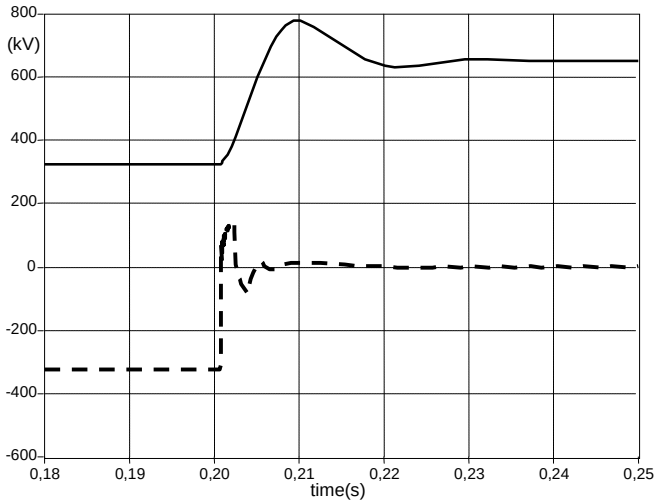

Fig. 12. DC cable fault at the line end: healthy pole (solid line) and faulted pole (dashed line) voltages to ground at the nearby converter station, vs. time. No dc side MOSAs.

Two alternate MOSA arrangements were simulated:

a) U_r=360 kV, 8 parallel columns
b) U_r=390 kV, 6 parallel columns

Simulation results, obtained for a conservatively assumed fault elimination (ac circuit breaker tripping) time of 0.3 s, are shown in Fig. 13.

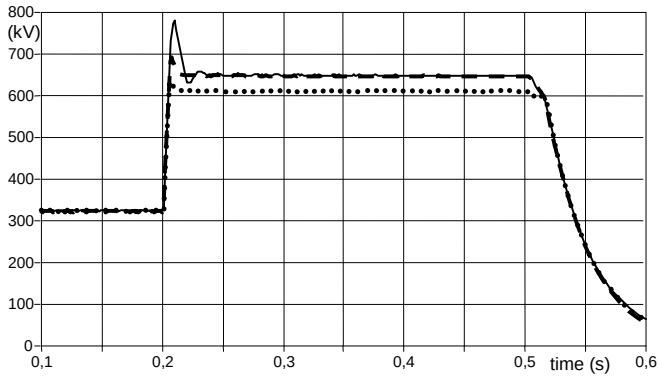

Fig. 13. DC cable line-end fault; healthy pole voltages to ground at the nearby converter station, for different MOSA arrangements, vs time. Solid line: no MOSAs; dotted line: 8×360 kV MOSA (alt. a in the text); dashed line: 6×390 kV MOSAs (alt. b in the text)

The two solutions differ markedly, as higher rated MOSAs (alt. b) only clip the initial transient spike, whereas lower rated ones (alt. a) also reduce the sustained overvoltage to 1.88 p.u.(602 kV), from the initial 2.03p.u. (650 kV) value (see Fig. 13). Moreover, the steady-state fault current increases as MOSAs connected to the sound cable, offer a further reclosing path to the fault current injected into the ground, as shown in Fig. 14. The peak value (i.e. the capacitive discharge) is not affected by SAs, whereas the dc component that flows mainly in the ground increases significantly, and ac components, reclosing through the sheath of the faulted cable (i.e. following

the loop having the lowest reactance) do not significantly change. This can be regarded as another check of the good response of the Finite Section modeling technique.

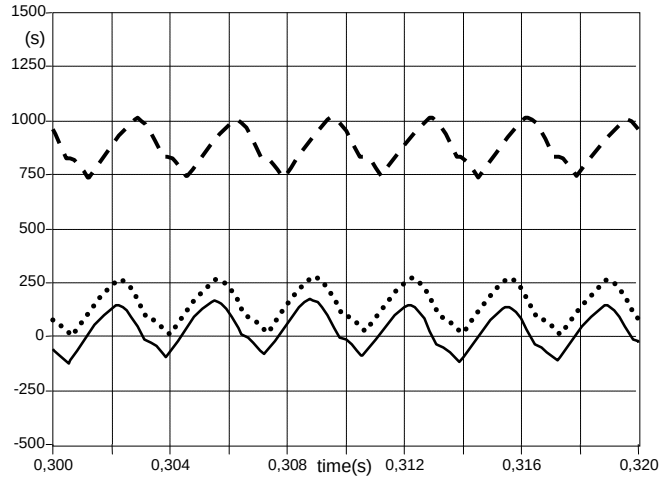

Fig. 14. DC cable line-end fault current, for different MOSA arrangements, vs time: Solid line: no MOSAs; dashed line 8×360 kV MOSAs (alt. a); dotted line: 6×390 kV MOSAs (alt. b)

The key factor for choosing between alternatives a) and b) is given by the energy absorption duty of simulated MOSAs, shown in Fig. 15. The energy absorbed by a single 360 kV column (alt. a) reaches 10.5 MJ, a destructive level even for class 5 arresters; 390 kV arresters (alt. b) are much less stressed at a tolerable 2.5 MJ, but on the other hand they are practically ineffectual against the TOV. Given the sustained nature of the latter, its reduction is not possible with standard arresters: application requirements resemble instead those of MOSAs for series capacitor banks protection. The question deserves further investigation.

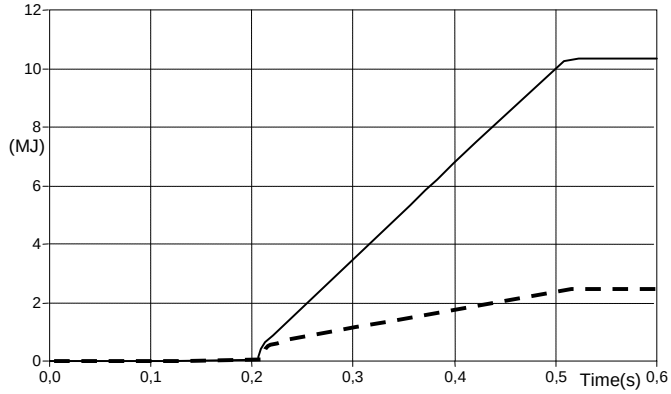

Fig. 15. Dc cable line-end fault: energy absorption in one MOSA column, vs time. Solid line: U_r=360 kV (alt. a); dashed line: U_r=390 kV(alt. b)

VII. Induced voltage on nearby circuits.

In the 13 km long tunnel stretch of the line route, the HVDC cables run parallel to LV auxiliary (safety) cable circuits. The voltage induced in such circuits by HVDC cable fault currents, must be evaluated in order to decide the minimum installation distance between HVDC and LV cables and, in case, take some measures to protect the LV circuits (SPDs, cable shielding…). Furthermore, in normal operation, the converter injects small non-characteristic low-order current harmonics on the dc side, whose effect should also be evaluated.

Basically two approaches can be applied:

- Frequency domain analysis
- Time domain analysis

The first method implies Fourier transformation of the short circuit current waveform (obtained by time-domain simulation), calculation of frequency components of induced voltage and then inverse Fourier transformation. The second method only requires adding the parallel LV cable, on which induced voltages are calculated, into the time-domain simulation model. This has been easily done with the Finite Sections approach, simulating the presence of a single core 2.5 mm^2 LV cable installed at different distances from the HVDC cables. Simulation results evidence considerable impulsive overvoltages for close installation (Fig. 14, around 500 V/km at 0.5 m), quickly decreasing with time to a few volt per km, as shown in Fig. 16. Given a 4 kV insulation level for the LV cable, and assuming it is 13 km long, installation distance must be at least 2.5 m. In practice, countermeasures will be most likely adopted at LV level, given the physical constraint on spacing imposed by tunnel installation.

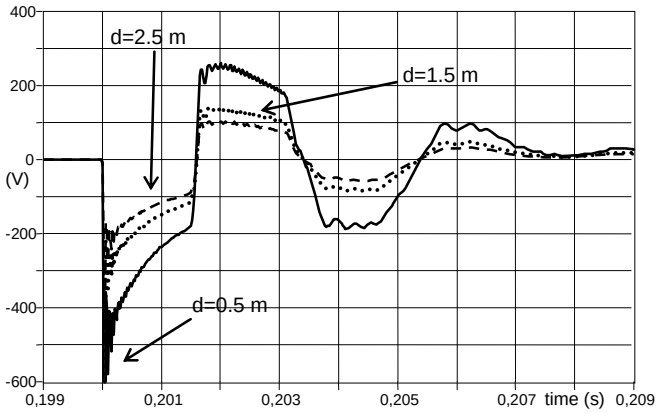

Fig. 16. Transient overvoltage induced in 1km of LV cable laid along the dc line at different distances; d=0.5 m (solid line), d=1.5m (dotted line) and d=2.5 m (dashed line), vs time.

VIII. Conclusions

The ATP-EMTP short circuit transient study of a planned 200 km long HVDC-VSC underground cable link, including detailed "Finite Sections" modeling of HVDC cables, including tunnel installation, was presented. Simulation results show that:

- steady state currents for dc pole-to-ground, actually cable core to sheath, faults are very small (a few tens of Amps), due to high-impedance ac neutral grounding on the converter side of transformers and absence of dc grounding.
- The initial value of fault current is however much higher (tens of kA) due to the discharging capacitance of the 200 km-long cable; although peak value and specific energy I^2t of the fault current do not endanger the cable

sheaths.

- In case of pole-to-ground dc faults the healthy cable is affected by a sustained (temporary) overvoltage reaching 2.0 p.u. due to operation with ac neutral high impedance grounded and dc ungrounded.
- Control of such overvoltages by MOSAs requires very high energy absorption capability, even within normal operating times of ac side tripping of circuit breakers. MOSAs are moreover found to increase significantly the steady state fault current.
- Transient overvoltages induced on adjacent circuits can be of concern. Proper spacing between HVDC and parallel LV circuits is to be foreseen, along with installation on the latter of SPDs.

The simulated 2 p.u. healthy pole overvoltage is not specific to the selected VSC design: it is indeed a common feature of balanced VSC-HVDC transmission systems in case of dc line (cable) fault, as recently stated in [8]. On the other hand, current waveforms at converter stations are dependent on the actual converter topology.

Finite Sections cable modeling allows accurate representation and analysis of phenomena of interest; further developments include the optimization of MOSAs protection level and energy absorption capability.

IX. REFERENCES

[1] *TERNA development plan 2010*, available online www.terna.it

[2] F. Palone, L. Colla and S. Lauria, "HVDC-VSC Short Circuit Calculation Using Finite Section Cable Modeling," in *Proc. 2010 EEUG Meeting*, Helsinki (Finland), Aug. 2010.

[3] ATPDRAW version 3, *User Manual*, TR A4389, EFI, Norway, 1996

[4] R. J. Meredith, "EMTP Modelling of electromagnetic transients in multi-mode coaxial cables by finite sections," *IEEE Trans. Power Delivery*, vol. 12, pp. 489-497, Jan. 1997.

[5] L. Colla, S. Lauria, F. Palone, "*Finite Sections Modeling of Power Cable Systems*" accepted for presentation at IPST 2011 (paper 139), Delft, the Netherlands, June 2011.

[6] Canadian-American EMTP Users Group, "ATP-EMTP Rule Book, 1997.

[7] CEI (Italian Electrotechnical Committee) 103-6 *"Protection of communication lines from induction effects due to fault on nearby power lines"* (in Italian), 1997

[8] CIGRE Working Group B4.48, "Components testing of VSC system for HVDC application", CIGRE Technical Brochure 447, Feb. 2011